New neutron-deficient Pb and Bi nuclides produced in cross bombardments with heavy ions

Y. Le Beyec, M. Lefort, and J. Livet
Laboratoire de Chimie Nucléaire, Institut de Physique Nucléaire, 91406-Orsay, France

N. T. Porile*
Department of Chemistry, Purdue University, Lafayette, Indiana 47906

A. Siivola
Department of Physics, University of Helsinki, Finland, and Lawrence Berkeley Laboratory, Berkeley, California 94720

(Received 9 July 1973)

New α-emitting bismuth nuclides ranging in mass number from 189 to 197 and lead nuclides ranging from 186 to 192 have been produced in the following reactions: ^{203}Tl(^{3}He,xn)$^{206-x}$Bi, ^{187}Re(^{16}O,xn)$^{205-x}$Bi, ^{185}Re(^{16}O,xn)$^{203-x}$Bi, ^{181}Ta(^{20}Ne,xn)$^{201-x}$Bi, ^{159}Tb(^{40}Ar,xn)$^{199-x}$Bi, ^{181}Ta(^{19}F,xn)$^{200-x}$Pb, ^{182}W(^{16}O,xn)$^{198-x}$Pb, and ^{155}Gd(^{40}Ar,xn)$^{195-x}$Pb. Assignments were made on the basis of excitation function measurements and comparison with similar reactions leading to the formation of the analogous well-known Po nuclides. The following assignments were made, where for each nuclide the two listed numbers are the α-ray energy in MeV and half-life: ^{197}Bi^{m}—5.77, 10 min; ^{195}Bi—5.43, 170 sec; ^{195}Bi^{m}—6.11, 90 sec; ^{194}Bi—5.61, 105 sec; ^{193}Bi—5.90, 64 sec; ^{193}Bi^{m}—6.18; ^{192}Bi—6.06, 42 sec; ^{191}Bi—6.32, 13 sec; ^{191}Bi^{m}—6.63; ^{191}Bi^{m}—6.86; ^{190}Bi—6.45, 5.4 sec; ^{189}Bi—6.67, <2 sec; ^{192}Pb—5.06, 2.3 min; ^{191}Pb—5.29, 1.3 min; ^{190}Pb—5.58, 1.2 min; ^{189}Pb—5.72, 51 sec; ^{188}Pb—5.98, 26 sec; ^{187}Pb—6.08, 17 sec; and ^{186}Pb—6.32, 8 sec. Estimates of α branching ratios are also presented.

[RADIOACTIVITY new nuclides ^{197}Bi^{m}, ^{195}Bi, ^{195}Bi^{m}, ^{194}Bi, ^{193}Bi^{m}, ^{192}Bi, ^{191}Bi, ^{191}Bi^{m}, ^{190}Bi, ^{189}Bi, ^{192}Pb, ^{191}Pb, ^{190}Pb, ^{189}Pb, ^{188}Pb, ^{187}Pb, ^{186}Pb; nuclides produced in various (HI,xn) reactions; measured E_{α}, $t_{1/2}$, α branching ratios.]

I. INTRODUCTION

Some years ago, Siivola[1] presented preliminary results on α decay of several bismuth and lead isotopes of masses lighter than 197. Similar data were obtained later for a number of bismuth isotopes by Tarantin, Kabachenko, and Demyanov.[2] More recently ^{3}He and ^{40}Ar irradiations carried out at Orsay have produced many of the neutron-deficient Pb and Bi nuclei. The results have confirmed the previous ones and new data have become available.[3] In this paper we present a joint report of the work on these nuclides done at Berkeley with ^{16}O, ^{19}F and ^{20}Ne ions,[1] and that performed at Orsay with ^{3}He and ^{40}Ar ions.[3]

Excitation functions will be presented for the following reactions: ^{159}Tb(Ar,xn), ^{155}Gd(Ar,xn), ^{181}Ta(^{20}Ne,xn), ^{181}Ta(^{19}F,xn), ^{185}Re(^{16}O,xn), ^{182}W(^{16}O,xn), ^{206}Pb(^{3}He,xn), and ^{203}Tl(^{3}He,xn). From the study of their thresholds and maxima, it is possible to make mass assignments for the nuclides which are responsible for the observed α spectra. Comparisons with several excitation functions yielding the corresponding Po nuclides were also helpful in this respect. The results of half-life and α-branching determinations will also be given.

II. EXPERIMENTAL

A. Irradiations

Beams of ^{16}O, ^{19}F, and ^{20}Ne ions were delivered at the HILAC (Berkeley) at a maximum energy of 10.4 MeV/amu. 300-MeV ^{40}Ar ions were obtained from the accelerator ALICE at Orsay. Aluminum foils were used to degrade the energy to between 150 and 300 MeV for ^{40}Ar and to the energy range 100–200 MeV for the other ions.

The bombarding energy at the target was calculated with the aid of Northcliffe's tables.[4] Absolute intensity measurements were made with Faraday cups, whenever the ions from the beam could be collected after passing through the target. When the experimental setup for collecting the recoiling products prevented the placement of a Faraday cup in the beam during irradiation, a metallic grid was placed in front of the target and a partial beam current was measured. Calibrations of the grid relative to the Faraday cup were made immediately before and after the irradiations. Intensities of the order of 5×10^{10} Ar ions per second and more than 10^{11} oxygen and neon ions were commonly used.

A beam of ^{3}He ions was delivered by the Orsay

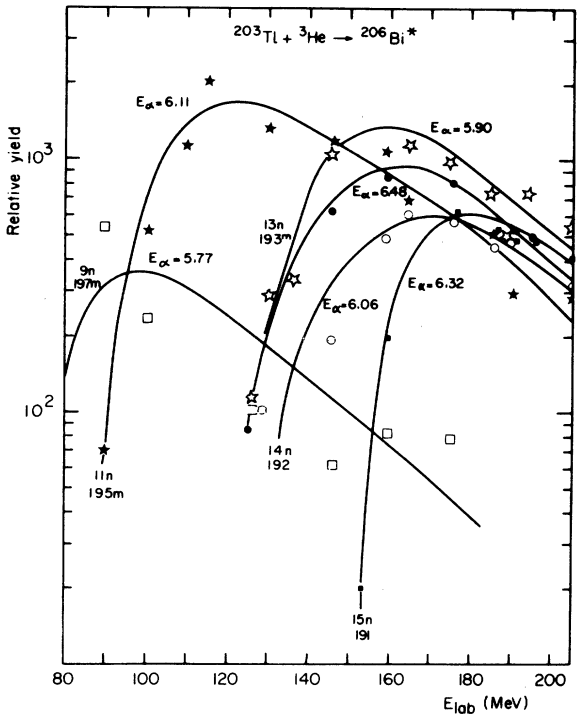

FIG. 1. Excitation functions for the reactions ^{203}Tl-(^{3}He, xn)$^{206-x}$Bi. Relative yield refers to the observed α counting rate at equilibrium.

synchrocyclotron at 210 MeV. Energies between 100 and 200 MeV were obtained by degrading the beam with copper foils and applying Williamson and Boujot's[5] data for the stopping power. The intensity, about 10^{11} ions per second, was measured during bombardment with a thin helium gas ionization chamber through which the beam passed before hitting the target. The ionization chamber had previously been calibrated at several energies against a Faraday cup.

B. Targets

For ^{3}He bombardment, ^{206}Pb (enriched to 94.9%) and ^{203}Tl (97.4%) were prepared at the Atomic Energy Research Establishment (Harwell) with a thickness of 1 mg/cm^2 by evaporation onto a 3 μm aluminum backing. A ^{155}Gd (94.3%) target was made by the painting technique to a thickness of approximately 1-mg/cm^2 Gd_2O_3 on aluminum backing. ^{149}Tb was prepared by electrophoresis of Tb_2O_3. The Ta target consisted of a self-supporting foil (10.6 mg/cm^2). Rhenium isotopes were electroplated onto a 2.3-mg/cm^2 Ni foil. The thicknesses were 0.56 mg/cm^2 for ^{185}Re (96.7%) and 0.67 mg/cm^2 for ^{187}Re (99.2%). Tungsten isotopes, ^{180}W (11.4%) and ^{182}W (94.4%), were painted as WO_3 on similar Ni backings. Their effective thickness is uncertain (2–4 mg/cm^2).

C. Detection of α emitters

Neutron-deficient isotopes of lead and bismuth decay partially by α emission and were detected by α spectroscopy. The α energies increase with neutron deficiency and the corresponding half-lives decrease. In order to transfer products with half-lives of the order of seconds to the vicinity of a counter, a fast transport technique is required. In this work we used the well-known helium jet technique[6] previously described for the case of ^{16}O and ^{20}Ne bombardments, where it was adapted for half-lives longer than 1 sec. At Orsay, the helium jet apparatus is able to collect and transport recoils in a time less than a few msec.[7]

For the reactions induced by ^{3}He, ^{16}O, and ^{20}Ne the distance between the target and the capillary through which the ejected recoils were swept out by the helium flow was set to slightly exceed the recoil range in helium. In the case of the Ar-induced reactions this distance had to be varied with

TABLE I. Comparison of (^{3}He, xn)-induced reactions on ^{206}Pb and ^{203}Tl which produce Po and Bi isotopes.

x	Isotope	Threshold [$E_{lab}+\Delta Q$ (Po-Bi)]	Energy at the peak	Widths of the excitation function (ΔE_{lab})	Relative intensity at the peak
9	^{200}Po	~70 MeV	98 MeV	···	100
	^{197}Bi^m $E_\alpha = 5.77$	~70 MeV	100 MeV	45 MeV	1.8
11	^{198}Po	90 MeV	125 MeV	50 MeV	12
	^{195}Bi^m $E_\alpha = 6.11$	90 MeV	125 MeV	55 MeV	7
13	^{196}Po	118 MeV	158 MeV	65 MeV	1.6
	^{193}Bi $E_\alpha = 5.90$	120 MeV	160 MeV	62 MeV	0.8
	^{193}Bi^m $E_\alpha = 6.48$			65 MeV	0.5
14	^{195}Po	130 MeV	175 MeV	78 MeV	0.7
	^{192}Bi $E_\alpha = 6.06$	130 MeV	172 MeV	70 MeV	0.03

the bombarding energy because of the large variation in the recoil ranges. The ranges were calculated according to Northcliffe[4] and the actual target-to-capillary distance was set at 1.5 times the range to reflect the previously determined[7] optimum collection efficiency.

The various reaction products were transported to the vicinity of a silicon surface-barrier detector and α spectra were recorded. The α-ray energy calibration was made with ^{244}Cm, ^{252}Cf, and the active deposit of thoron. Their energies were taken from the literature.[8] Half-life measurements were made by repeating the irradiation-counting sequence many times (multispectrum technique). The decay curves were computer-analyzed by the least-squares method.

III. RESULTS FOR BISMUTH ISOTOPES

A. Excitation functions

Most of the bismuth nuclei studied in this work have been produced by three or four different reactions. Below we shall present the observed excitation functions.

1. ^{3}He-induced reactions

Reaction cross sections for ^{203}Tl(^{3}He, xn)$^{206-x}$Bi were measured over a wide energy range. ^{203}Tl and ^{206}Pb targets were irradiated exactly under the same experimental conditions and therefore, by comparing each excitation function with the corresponding excitation functions for ^{206}Pb(^{3}He, xn)$^{209-x}$Po, where the well-known polonium isotopes for x between 9 and 15 are produced, it has been possible to decide to which particular isotope of Bi an observed α group belongs. The excitation functions for the formation of bismuth nuclides ranging from ^{197}Bi to ^{191}Bi are plotted in Fig. 1. Table I shows a comparison of (^{3}He, xn)-induced reactions on ^{206}Pb and ^{203}Tl which produce the Po and Bi isotopes. A correction ΔQ which takes into account the differences in Q values has been applied to the Bi curves in order to obtain the energy values which appear in this table.

Since the Tl and Pb targets were thicker than the recoil ranges only a fraction of the recoils escaped from the target. As this fraction varies with bombarding energy a correction had to be made. The recoil ranges, which correspond to the effective target thickness, were calculated at each bombarding energy by means of Northcliffe's tables[4] and the cross sections corrected for the difference between the range obtained at a given energy and at 100 MeV.

2. ^{16}O- and ^{20}Ne-induced reactions

In Figs. 2 and 3, excitation functions are shown for (^{16}O, xn) reactions, where $6 \leq x \leq 10$, on ^{185}Re

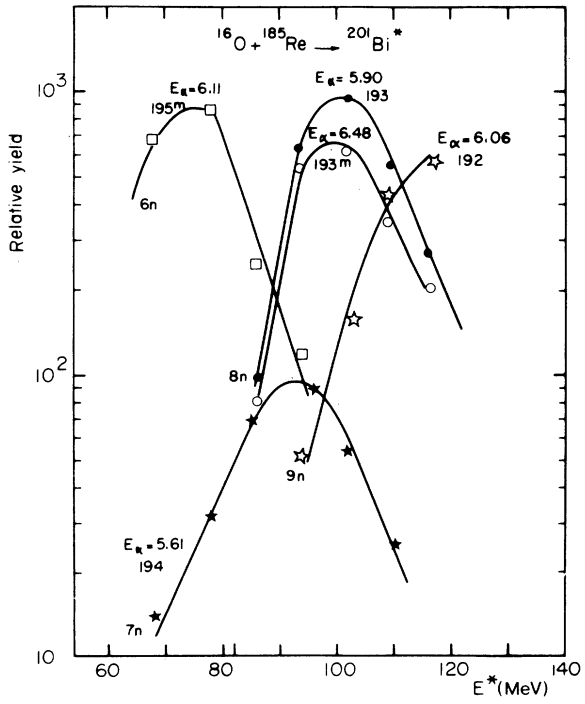

FIG. 2. Excitation functions for the reactions ^{185}Re-(^{16}O, xn)$^{201-x}$Bi. E^* is the initial excitation energy of the compound nucleus.

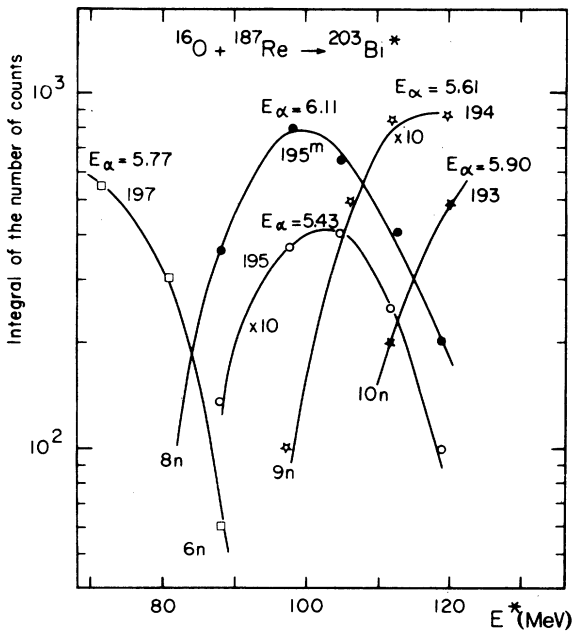

FIG. 3. Excitation functions for the reactions ^{187}Re-(^{16}O, xn)$^{203-x}$Bi. A different ordinate scale applies to each curve in this figure.

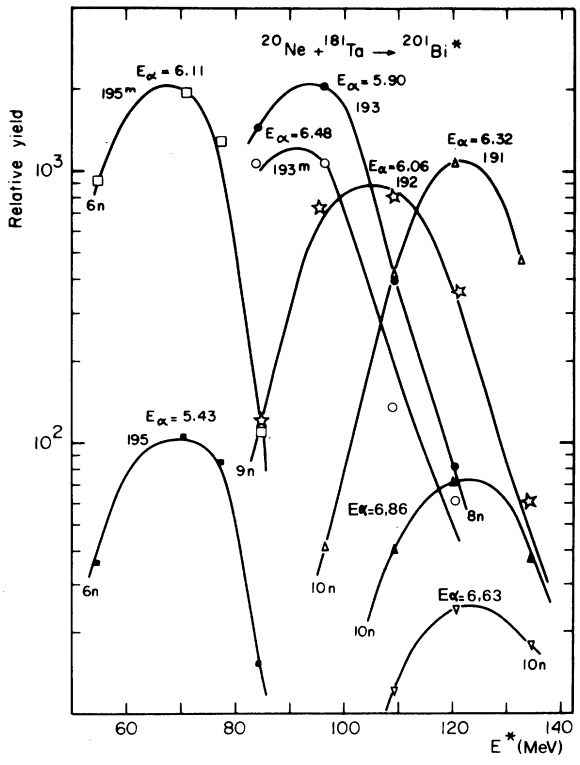

FIG. 4. Excitation functions for the reactions ^{181}Ta-$(^{20}$Ne, $xn)^{201-x}$ Bi.

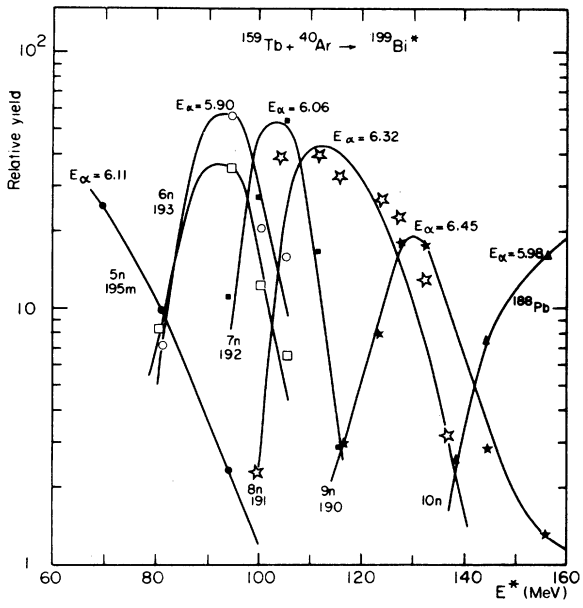

FIG. 5. Excitation functions for the reactions ^{159}Tb-$(Ar, xn)^{199-x}$Bi.

and ^{187}Re targets, respectively.

Figure 4 shows excitation functions for similar xn reactions induced by ^{20}Ne in ^{181}Ta. The results for both Re and Ta targets were corrected for the variation of the effective target thickness with bombarding energy in the manner described above. Concerning the Ta target, most of the foil acted as a beam degrader. This fact was taken into account in the calculation of the excitation energies of the compound system.

3. *^{40}Ar-induced reactions*

Excitation functions for the reactions ^{151}Tb-$(Ar, xn)^{199-x}$ Bi are given in Fig. 5. A comparison is made in Table II between ^{164}Dy$(Ar, xn)^{204-x}$ Po

TABLE II. Comparison of $(^{40}Ar, xn)$-induced reactions on ^{164}Dy, ^{149}Tb, and ^{155}Gd which produce isotopes of Po, Bi, and Pb.

x	Isotope	Threshold excitation energy $+\Delta$ Sn (Po-Bi) or Δ Sn (Po-Pb)	Energy at the peak	Width of the excitation function	Relative intensity at the peak
6	^{198}Po	≃73 MeV	90 MeV	···	100
	^{193}Bi $E_\alpha = 5.90$				7
	^{193}Bi^m $E_\alpha = 6.48$	75 MeV	90 MeV	17 MeV	3
	^{189}Pb $E_\alpha = 5.72$	···	88 MeV	···	1.5
7	^{197}Po^m	85 MeV	104 MeV	15 MeV	60
	^{192}Bi $E_\alpha = 6.06$	85 MeV		14 MeV	5
	^{188}Pb $E_\alpha = 5.98$	85 MeV		15 MeV	0.6
8	^{196}Po	97 MeV	115 MeV	17 MeV	20
	^{191}Bi $E_\alpha = 6.32$	97 MeV		≃19 MeV	4
	^{187}Pb $E_\alpha = 6.08$	97 MeV		≃20 MeV	0.6
9	^{195}Po^m	≃105 MeV	128 MeV	17 MeV	5
	^{190}Bi $E_\alpha = 6.45$	≃105 MeV		15 MeV	2
	^{186}Pb $E_\alpha = 6.32$	≃105 MeV		···	0.14

reactions, for which all the polonium nuclei are well known, and the ^{159}Tb(Ar, xn)$^{199-x}$Bi reactions. In order to make a direct comparison for a given x, between the energy values at the reaction threshold and at the maximum of excitation functions, the excitation functions of the bismuth isotopes were shifted by the difference between neutron binding energies for x neutrons, starting from ^{204}Po in one case and ^{199}Bi in the other.

B. Mass assignments

All the measured excitation functions have a shape corresponding to a compound-nucleus mechanism. A given α ray appears at a threshold energy; then at higher energies its intensity increases, goes through a maximum, and decreases when a new α ray appears and begins to increase in intensity. The energy shift between two adjacent thresholds or maxima varies between 12 and 15 MeV and corresponds to the additional total energy needed for the evaporation of an extra neutron.

In order to ascertain whether any of the observed α rays belonged to an isotope of a lighter element such as Pb or Tl, reactions ^{155}Gd(Ar, xn)$^{195-x}$ Pb as well as ^{181}Ta(^{19}F, xn)$^{200-x}$ Pb were also studied. None of the α rays attributed to Bi isotopes were observed for these targets.

The following assignments were made:

1. $^{197}Bi^{m}$: $E_\alpha = 5.77$ MeV, $t_{1/2} \sim 10$ min

A comparison of the excitation function of the reaction (^{3}He, $9n$) induced on ^{206}Pb with that of the 5.77-MeV α ray appearing in the bombardment of ^{203}Tl shows that this group corresponds to the production of $^{206-9}$Bi. This is confirmed by the observation of the same α ray in the ^{187}Re(^{16}O, xn)-$^{207-x}$Bi reaction. The excitation function is not inconsistent with a (^{16}O, $6n$) reaction although it was not completely determined. However, α systematics indicate that decay from the ground state of ^{197}Bi should correspond to a somewhat lower value than 5.77 MeV. Since isomeric states are observed for all bismuth nuclei with even N, it is reasonable to assume that the observed α ray is due to a metastable level.

2. ^{196}Bi

No α branching was observed for this nuclide regardless of the entrance channel (^{3}He, Ar, O, or Ne).

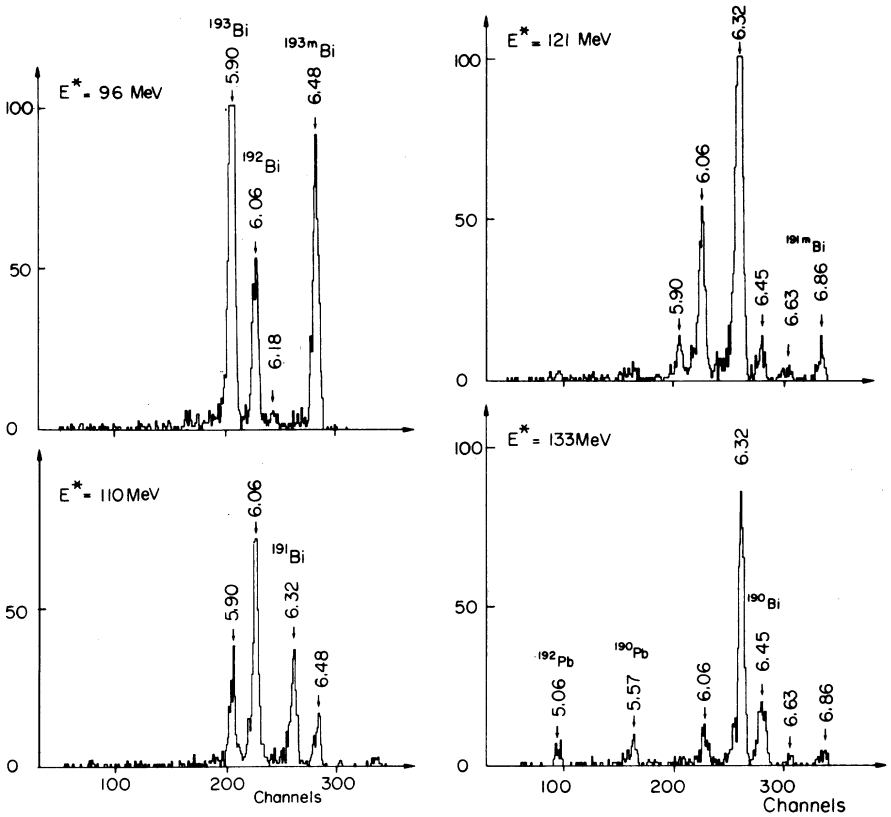

FIG. 6. α spectra of Bi activities produced in ^{20}Ne + ^{181}Ta bombardments at various energies.

3. ^{195}Bi *and* $^{195}Bi^m$:
$E_\alpha = 5.43 \pm 0.01$ MeV, $t_{1/2} = 170 \pm 20$ sec
$E_\alpha = 6.11 \pm 0.01$ MeV, $t_{1/2} = 90 \pm 5$ sec

When a comparison is made between the excitation function for the $^{206}Pb(^3He, 11n)^{198}Po$ reaction and that for the 6.11-MeV α ray produced by ^3He on ^{203}Tl, it follows very clearly that the latter corresponds to the evaporation of 11 neutrons from ^{206}Bi. The same activity is produced by bombardment of ^{185}Re by ^{16}O and also of ^{181}Ta by ^{20}Ne, as shown in Figs. 2 and 4. These excitation functions are consistent with $(^{16}O, 6n)$ and $(^{20}Ne, 6n)$ reactions, respectively, both of which yield ^{195}Bi. In addition to the 6.11-MeV α ray, a 5.43-MeV group with a substantially longer half-life was also observed. Its excitation function is similar to that of the 6.11-MeV α ray although its intensity is some 20 times lower. This 5.43-MeV radiation could not be observed in ^3He-induced reactions. On the basis of α systematics, it seems reasonable to attribute the 6.11-MeV α ray to the decay of an isomeric state of ^{195}Bi and the 5.43-MeV group to that of the ground state.

4. ^{194}Bi: $E_\alpha = 5.61 \pm 0.02$ MeV, $t_{1/2} = 105 \pm 15$ sec

A ray at 5.61 MeV appeared in the α spectra for excitation energies above 65 MeV in the ^{16}O-induced reaction on ^{185}Re (Fig. 2). The corresponding excitation function indicates that seven neutrons should be emitted. However, the yield is approximately 10 times smaller than observed for the $(^{16}O, 6n)$ reaction. This radiation was not observed in the ^3He-induced reactions, probably because of its low intensity.

5. $^{193}Bi^m$: $E_\alpha = 6.48 \pm 0.01$ MeV
$E_\alpha = 6.18 \pm 0.02$ MeV (4%)
$(t_{1/2} = 3.5 \pm 0.2$ sec)
^{193}Bi: $E_\alpha = 5.90 \pm 0.01$ MeV,
$(t_{1/2} = 64 \pm 4$ sec)

Here again, two identical excitation functions were observed for 6.48- and 5.90-MeV α groups in the bombardment of ^{185}Re by ^{16}O and that of ^{181}Ta by ^{20}Ne. These peaks were seen at higher energies than ^{194}Bi and the emission of eight neutrons is the most reasonable assumption. As in the case of ^{195}Bi, two isomeric states should be considered. Excitation functions attributed to $(^3He, 13n)$ are characterized by the same radiations. A comparison made with the $^{206}Pb(^3He, 13n)^{196}Po$ reaction strongly supports this assignment. Further evidence for the assignment of these groups to ^{193}Bi comes from their production in argon-induced reactions. Table II shows that the energies of the threshold and maxima are comparable to that of ^{198}Po formed in the $^{164}Dy(Ar, 6n)$ reaction, so that they correspond to the $^{159}Tb(Ar, 6n)^{193}Bi$ reaction. In addition to these two main groups, there is a weak group at 6.18 MeV whose intensity is ~4% of that of the 6.48-MeV group. It may be a fine-structure group belonging to $^{193}Bi^m$.

6. ^{192}Bi: $E_\alpha = 6.06 \pm 0.01$ MeV, $t_{1/2} = 42 \pm 5$ sec

The $^{181}Ta(Ne, 9n)^{192}Bi$ reaction occurs at higher energies than the $(Ne, 8n)$ reaction. Moreover, the excitation functions for the production of the 6.06-MeV α ray in $^{203}Tl(^3He, xn)$ and $^{159}Tb(Ar, xn)$ reactions were compared with those of the ^{206}Pb-$(^3He, 14n)^{195}Po$ and $^{164}Dy(Ar, 7n)^{197}Po$ reactions, respectively. These comparisons clearly lead to the conclusion that ^{192}Bi decays through the 6.06-MeV α ray, as shown in Tables I and II.

7. ^{191}Bi: $E_\alpha = 6.32 \pm 0.01$ MeV,
$(t_{1/2} = 13 \pm 1$ sec)
$^{191}Bi^m$: $E_\alpha = 6.63 \pm 0.02$ MeV (30%)
$E_\alpha = 6.86 \pm 0.02$ MeV (70%)
$(t_{1/2} = 20 \pm 15$ sec)

Table II shows very clearly that ^{191}Bi is produced in the reaction $^{159}Tb(Ar, 8n)$ and decays by the emission of 6.32-MeV α rays. The same energy

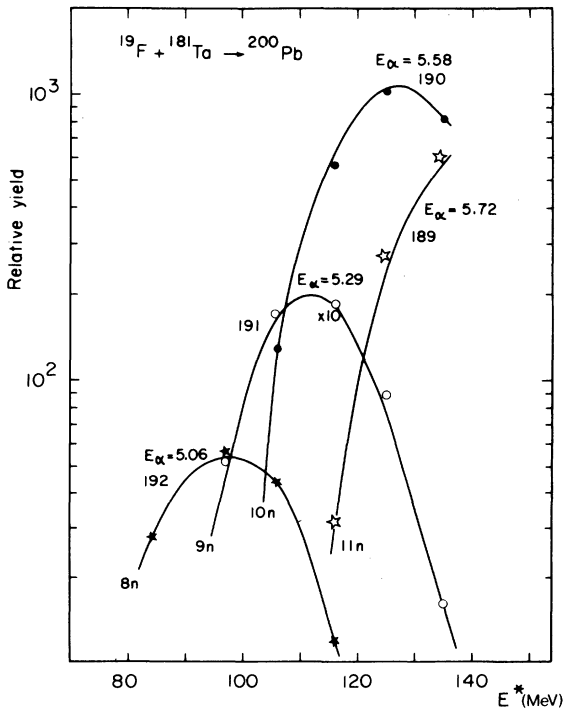

FIG. 7. Excitation functions for the reactions ^{181}Ta-$(^{19}F, xn)^{200-x}Pb$.

group was observed, as shown in Fig. 4, in the ^{181}Ta(^{20}Ne, 10n) reaction. In addition, for this case, two other α rays at 6.63 and 6.86 MeV were observed in the α spectra (Fig. 6), in the same bombarding energy range.

Figure 4 shows that these two α rays should also be attributed to ^{191}Bi. The intensities are substantially lower than that of the 6.32-MeV α ray, the relative values being 1, 0.12, and 0.05, in order of increasing energy. The 6.63-MeV peak was not observed in the argon-induced reactions because the beam intensity was roughly 15 times lower than that of the neon beam, and also, the cross section for complete fusion without fission is smaller for Ar than for Ne.

8. ^{190}Bi: $E_\alpha = 6.45 \pm 0.01$ MeV, $t_{1/2} = 5.4 \pm 0.5$ sec

In the ^{181}Ta(^{20}Ne, xn)$^{201-x}$Bi reaction series (Fig. 6), an α ray of 6.45 MeV appears at approximately 15 MeV above the threshold of the reaction ^{181}Ta-(Ne, 10n)^{191}Bi. Also, excitation functions of Ar-induced reactions on ^{159}Tb clearly show (Table II) that the 6.45-MeV α ray corresponds to an (Ar, 9n) reaction, and should be attributed to ^{190}Bi.

9. ^{189}Bi: $E_\alpha = 6.67$ MeV ± 0.02, $t_{1/2} < 2$ sec

The reactions ^{159}Tb(Ar, xn) show that an α ray of 6.67 MeV appears at high excitation energies, above the threshold of the ^{159}Tb(Ar, 9n)^{190}Bi. In a recent paper,[9] a careful study of this excitation function demonstrated that the only possible assignment could be ^{189}Bi. Because of the low counting rate, the half-life could not be measured accurately, although one can assert an upper limit of 2 sec.

C. Limits for lighter bismuth isotopes

Presently, the lightest bismuth isotope which has been observed has $A = 189$. The use of ^{3}He-induced reactions makes it necessary to evaporate more than 15 neutrons in order to go further from stability. Because of fission competition it seems difficult to reach a lower limit. It would be more efficient to use reactions such as ^{180}W(^{19}F, 11n)^{188}Bi, ^{185}Re(^{16}O, 13n)^{188}Bi, and ^{181}Ta(^{20}Ne, 13n)^{188}Bi in the energy range around 200–240 MeV. This requires an accelerator delivering ^{16}O or ^{20}Ne beams at approximately 15 MeV per nucleon. In order to reach (Ar, 10n) with a reasonable number of events the actual beam intensity should be increased by an order of magnitude from the present value because, as discussed later, the fission-neutron emission competition becomes very severe for the high angular momenta which are reached. Furthermore, the proton binding energy[10] decreases to zero near $A = 189$, and there should be a large enhancement for proton emission to the detriment of neutron emission along the evaporation chain in the vicinity of this point.

IV. RESULTS ON LEAD ISOTOPES

A. Excitation functions for ^{19}F-, ^{16}O-, and ^{40}Ar-induced reactions

In Fig. 7, excitation functions are shown for the α emitters produced in ^{181}Ta(^{19}F, xn)$^{200-x}$ Pb reactions. They are very similar to the ^{185}Re(^{16}O, xn)-$^{201-x}$Bi excitation functions which were discussed previously and the mass assignments are straightforward. Figure 8 shows the excitation functions for the same α emitters produced in ^{182}W(^{16}O, xn)-$^{198-x}$Pb reactions. ^{155}Gd(^{40}Ar, xn)$^{195-x}$Pb and ^{164}Dy-(Ar, xn)$^{204-x}$Po results from the measured excitation functions are summarized in Table II.

B. Mass assignments for lead isotopes

α spectra are shown in Figs. 9 and 10, and exhibit α rays which have been attributed to Pb isotopes ranging in mass number from 192 to 186. The possibility that some of these groups could be due to Tl or Hg nuclides was eliminated on the

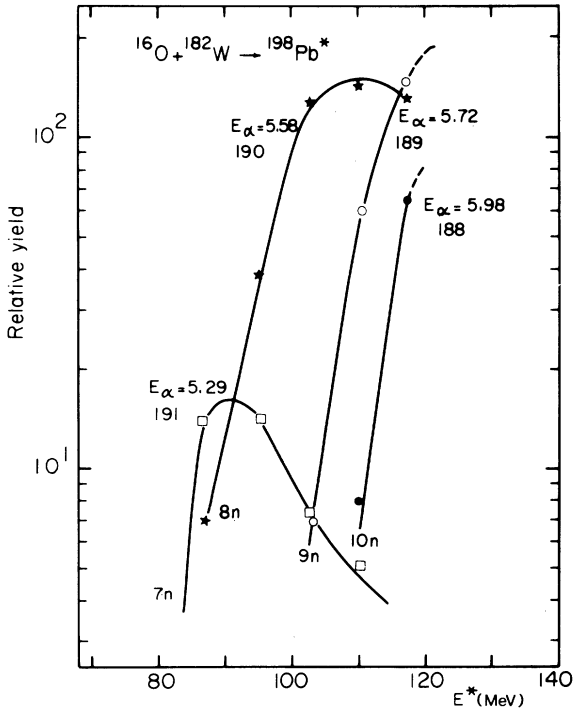

FIG. 8. Excitation functions for the reactions ^{182}W-(^{16}O, xn)$^{198-x}$Pb. Due to the uncertainty in the thickness of the WO_3 target, the E^* scale is uncertain by 5 MeV relative to Fig. 7.

basis of the shapes and peak positions of the excitation functions, which were in all cases characteristic of xn reactions. In addition, irradiations of ^{151}Eu and Sm by Ar ions failed to produce any of the α rays attributed to Pb isotopes so that the latter could not, in fact, be due to elements below lead.

1. ^{192}Pb: $E_\alpha = 5.06 \pm 0.03$ MeV, $(t_{1/2} = 2.3 \pm 0.5$ min)

In the case of Bi, the excitation energy necessary for the emission of eight neutrons was around 100 MeV. Since neutron binding energies for ^{192}Pb to ^{200}Pb are very close to binding energies for ^{193}Bi-^{201}Bi, one might deduce that at $E^* = 105$ MeV, the peak of the excitation function of the 5.06-MeV α ray obtained in the ^{181}Ta(^{19}F, xn)-induced reaction corresponds to $x = 8$, and therefore to ^{192}Pb.

2. ^{191}Pb: $E_\alpha = 5.29 \pm 0.02$ MeV, $(t_{1/2} = 1.3 \pm 0.3$ min)

This α ray was obtained in highest yield for an excitation energy of 120 MeV in the case of reactions induced in ^{181}Ta by ^{19}F ions. Also, in the ^{182}W(^{16}O, xn) series, the maximum occurred at an excitation energy of 90 MeV, corresponding to the emission of seven neutrons from the compound nucleus ^{198}Pb.

3. ^{190}Pb: $E_\alpha = 5.58 \pm 0.01$ MeV, $(t_{1/2} = 1.2 \pm 0.2$ min)

The α ray of 5.58 MeV was observed in ^{19}F-, ^{16}O-, and ^{40}Ar-induced reactions. The excitation energies at which the maximum yields were obtained indicated that x was equal to 10 for ^{19}F, 8 for ^{16}O, and 5 for ^{40}Ar. These values correspond to $A = 190$.

4. ^{189}Pb: $E_\alpha = 5.72 \pm 0.01$ MeV, $t_{1/2} = 51 \pm 3$ sec

The excitation functions for $E_\alpha = 5.72$ MeV are shifted to higher energies than those for $E_\alpha = 5.58$ MeV by approximately 13 MeV. Therefore the reactions leading to this group are assumed to be (^{19}F, $11n$) and (^{16}O, $9n$), both of which produce ^{189}Pb. In the case of ^{155}Gd(Ar, xn) reactions, although there were only three points measured on the excitation function $x = 6$ seems to be the most probable value.

5. ^{188}Pb: $E_\alpha = 5.98 \pm 0.01$ MeV, $t_{1/2} = 26 \pm 2$ sec

The excitation function of the 5.98-MeV α ray has been compared with that for the known reaction ^{164}Dy(Ar, $7n$)^{197}Po. Since both curves are very similar, there is no ambiguity in attributing $x = 7$ to Pb as well as to Po (see Table II).

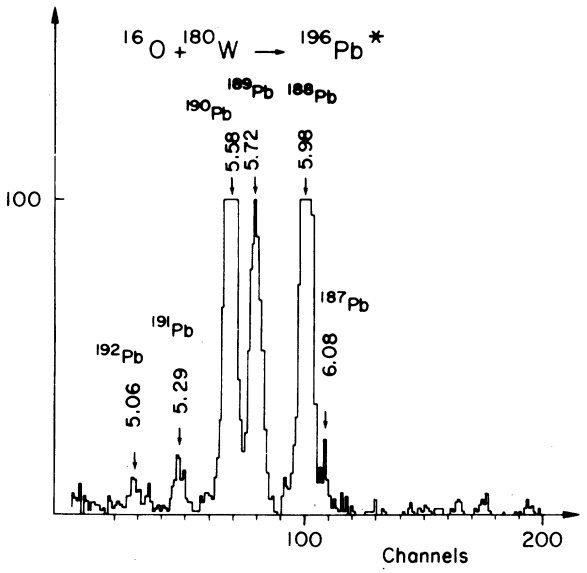

FIG. 9. An α spectrum of Pb activities from a ^{16}O + ^{180}W (11.4%) bombardment.

The same α ray was observed, but only slightly above threshold, for ^{182}W(^{16}O, $10n$).

6. ^{187}Pb: $E_\alpha = 6.08 \pm 0.02$ MeV, $t_{1/2} = 17 \pm 4$ sec

When bombarding ^{180}W by ^{16}o, an α ray of 6.08 MeV was observed, as shown in Fig. 9. A preliminary assignment was made to $A = 187$. Table II shows that strong confirmation for this assignment is obtained from the ^{155}Gd(Ar, $8n$) reaction.

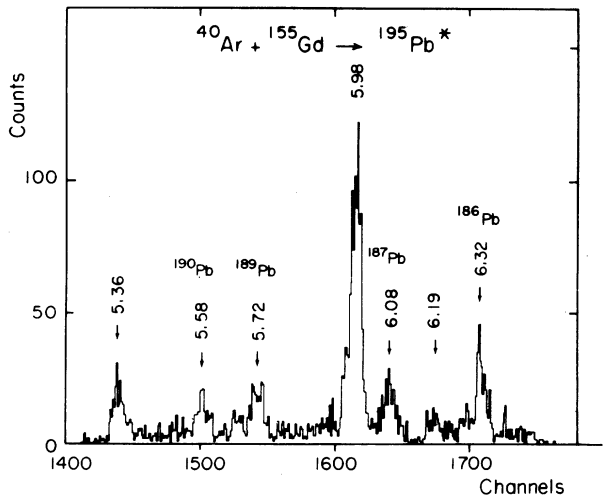

FIG. 10. An α spectrum of Pb activities from a ^{40}Ar + ^{155}Gd bombardment.

TABLE III. Comparison of $P(xn)$ values for Bi and Po isotopes.

x	$\frac{P(xn)\text{Po}}{P(xn)\text{Bi}}$	A of bismuth isotope	A of Po
6	2	193	198
7	2.2	192	197
8	1.95	191	196
9	2.7	190	195

7. ^{186}Pb: $E_\alpha = 6.32 \pm 0.02$ MeV, $t_{1/2} = 8 \pm 2$ sec

The threshold for the excitation function of the 6.32-MeV α ray is located at higher energies than the ^{155}Gd(Ar, $8n$)^{187}Pb reaction threshold. From comparison with ^{164}Dy(Ar, $9n$)^{195}Po, it was deduced in Table II that this α group is due to ^{186}Pb.

C. Limits for the production of light lead isotopes

For the moment, bombarding energies available for ^{16}O and ^{19}F(10 MeV/amu) are too low to reach x values large enough to produce lighter isotopes. With neon beams the ^{174}Hf(^{20}Ne, 9, 10n) reactions might be used to produce ^{184}Pb and ^{185}Pb. With Ar ions in the range of 7.5 MeV/amu, which are available at Orsay, one might expect to produce ^{185}Pb with a target of ^{154}Gd, instead of ^{155}Gd. With Ar ions of 10 MeV/amu, it would be possible to reach ^{184}Pb. Another very useful beam would be ^{40}Ca, since the bombardment of ^{144}Sm would produce a compound nucleus ^{184}Pb, and therefore, the possibility for the synthesis of lead isotopes around $A = 180$ would be open.

V. DISCUSSION OF α BRANCHING RATIOS AND α SYSTEMATICS

A. Branching ratios for α decay of Pb and Bi isotopes

Branching ratios were determined from a comparison of the intensities of the Bi and Pb α rays with those of the corresponding Po nuclides. The α-branching ratios of the latter have been measured[11] for polonium isotopes of A larger than 198. For the lighter nuclides, the branching ratios are very close to 100%.[12] Since we have measured, under exactly the same conditions, the (^{3}He, xn) excitation functions which yield either polonium or bismuth nuclei, a comparison can be made between the production yield of a given polonium isotope and that of the corresponding bismuth isotope. A similar comparison was made for (Ar, xn) reactions. If one assumes, for example, that $\sigma[^{164}\text{Dy}(\text{Ar}, 8n)^{196}\text{Po}] = \sigma[^{159}\text{Tb}(\text{Ar}, 8n)^{191}\text{Bi}]$ and knowing that ^{196}Po decays entirely by α emission, then the branching ratio for ^{191}Bi can be very simply deduced. This is true, of course, only if one believes that the fission-neutron evaporation competition is the same along both evaporation chains. We have done some calculations in order to check this assumption, starting from compound nuclei ^{204}Po and ^{199}Bi. It is known from recent works[13,14] that the evaporation probability of charged particles such as ^{4}He or ^{3}He is enhanced by high angular momentum values in the compound nucleus. Since particle binding energies along deexcitation chains, initial excitation energies, and angular momentum values were similar in both cases (polonium and bismuth), we assumed in these calculations the charged-particle evaporation competition to be almost the same, i.e.,

$$(\Gamma_f/\Gamma_n + \Gamma_f + \Gamma_{cp})_{\text{Po}} / (\Gamma_f/\Gamma_n + \Gamma_f + \Gamma_{cp})_{\text{Bi}} \simeq (\Gamma_f/\Gamma_n + \Gamma_f)_{\text{Po}} / (\Gamma_f/\Gamma_n + \Gamma_f)_{\text{Bi}}.$$

Although we cannot assert that the absolute Γ_f/Γ_n value is accurate, it is sufficient to compare Γ_f/Γ_n values obtained for bismuth and polonium isotopes.

It was found that the probability of reaching a nucleus after the emission of 6, 7, 8, and 9 neutrons from the compound nucleus ^{199}Bi is roughly 2 times

TABLE IV. Summary of results on Bi isotopes.

Nuclide	E_α (MeV)	$t_{1/2}$	Percent α decay
^{197}Bi^m	5.77	~10 min	0.1
^{196}Bi	...	...	...
^{195}Bi	5.43 ± 0.01	170 ± 20 sec	<0.2
^{195}Bi^m	6.11 ± 0.01	90 ± 5 sec	4
^{194}Bi	5.61 ± 0.02	105 ± 15 sec	<0.2
^{193}Bi^m	6.48 ± 0.01	3.5 ± 0.2 sec	25
^{193}Bi^m	6.18 ± 0.02		
^{193}Bi	5.90 ± 0.01	64 ± 4 sec	60
^{192}Bi	6.06 ± 0.01	42 ± 5 sec	20
^{191}Bi^m	6.63 ± 0.02	20 ± 15 sec	
^{191}Bi^m	6.86 ± 0.02		
^{191}Bi	6.32 ± 0.01	13 ± 1 sec	40
^{190}Bi	6.45 ± 0.01	5.4 ± 0.5 sec	90
^{189}Bi	6.67 ± 0.02	<2 sec	...

TABLE V. Summary of results on Pb isotopes.

Nuclide	E_α (MeV)	$t_{1/2}$	Percent α decay
^{192}Pb	5.06 ± 0.03	2.3 ± 0.5 min	...
^{191}Pb	5.29 ± 0.02	1.3 ± 0.3 min	...
^{190}Pb	5.58 ± 0.01	1.2 ± 0.2 min	...
^{189}Pb	5.72 ± 0.01	51 ± 3 sec	0.2
^{188}Pb	5.98 ± 0.01	26 ± 2 sec	1.5
^{187}Pb	6.08 ± 0.02	17 ± 4 sec	2.0
^{186}Pb	6.32 ± 0.02	8 ± 2 sec	2.4

smaller than the probability of reaching the corresponding final product from the compound nucleus ^{204}Po (Table III). Therefore the cross sections should be expected to be lower by a factor of 2. This result is based on the following calculations,[11] presented in the Appendix.

The α branching ratios of the bismuth nuclides were deduced from the measured polonium cross sections and the experimental bismuth α-ray intensities. The branching ratios of ^{193}Bi-^{190}Bi were based on the (Ar, xn) data and included the correction for differences in Γ_f/Γ_n values discussed above. The branching ratios of the heavier Bi nuclides were obtained from the (^{3}He, xn) data on the assumption that the ^{206}Pb(^{3}He, xn) and ^{203}Tl(^{3}He, xn) reaction cross sections were equal for a given x value. The results of this analysis, as well as the α-ray energies and the half-lives, are given in Table IV.

A similar calculation was performed for lead isotopes on the basis of the (Ar, xn) reaction data and the results are summarized in Table V.

B. α-decay systematics

The experimental α-decay energies may be compared with values derived from various mass formulas. Figure 11 shows a comparison with the values obtained from the reports by Myers and Swiatecki,[10] Garvey *et al.*,[15] and Zeldes, Grill, and Simievic.[16] It is apparent that the Myers and Swiatecki values give the best agreement with experiment while those of Garvey *et al.* differ by more than 1 MeV.

The experimentally observed trend of the α-decay energies can be extrapolated to presently unknown isotopes. On this basis we predict the following values: ^{185}Pb(Q_α = 6.6 MeV), ^{184}Pb(Q_α = 6.8 MeV, ^{188}Bi(Q_α = 7.0 MeV). These values are probably sufficiently accurate to be of help in the search for these isotopes.

APPENDIX

The ratio of the neutron and fission widths was calculated on the basis of the usual relationship[17]

$$\frac{\Gamma_n}{\Gamma_f} = \frac{4A^{2/3}}{a_n K_0} \frac{a_f(E - S_n - E_n)}{2[a_f(E - B_f - E_{R_f})]^{1/2} - 1} \times \exp\{2[a_n(E - S_n - E_R)]^{1/2} - 2[a_f(E - B_f - E_{Rf})]^{1/2}\}, \quad (1)$$

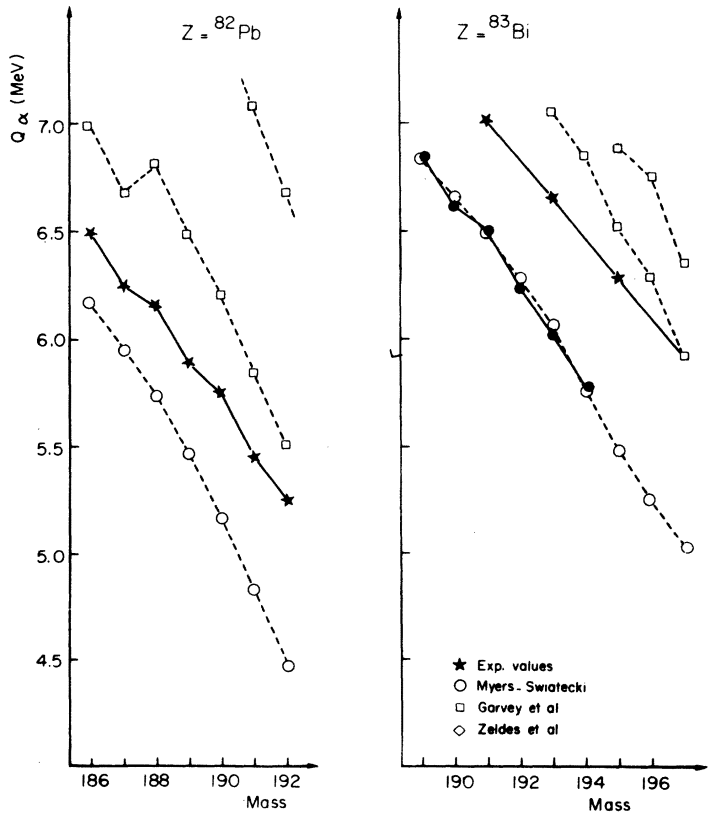

FIG. 11. A comparison of experimental α-decay energies, Q_α, and those calculated from various mass formulas.

where E is the excitation energy, S_n is the neutron binding energy, B_f is the fission barrier, a_f and a_n are the usual level density parameters for, respectively, the fissioning nucleus and the neutron-emitting nucleus, E_R is the rotational energy of the undeformed spherical nucleus, and E_{Rf} is the rotational energy at the fission saddle point. In a previous work[18] on the fission competition for polonium nuclei lighter than ^{210}Po, it was shown by Le Beyec and Lefort that the best values were 14.5 MeV^{-1} for a_f and 13 MeV^{-1} for a_n. S_n and B_f were taken from the Myers and Swiatecki tables.[10] E_R was calculated with the relation $E_R = \hbar^2 l(l+1)/2\mathcal{I}$, where $\mathcal{I}$, the moment of inertia, was that of a rigid rotor. The choice of the l distribution is rather difficult in the case of Ar-induced reactions. If complete fusion occurs for all angular momenta, a maximum value of $l \sim 174$ is obtained at a bombarding energy of 300 MeV, and the corresponding energy E_R is of the order of 100 MeV. However, it has been shown that l reaches a critical value beyond which compound nucleus formation does not occur. In the rare-earth region the limit for argon ions was found to be $l_{cr} \sim 130$. We have not put any limit in the calculations but it will be shown that this has no influence on the final results.

The rotational energy for the saddlepoint E_{Rf} is smaller than E_R. Describing the deformed shape as an ellipsoid, Huizenga[17] and Vandenbosch have shown that a ratio E_{Rf}/E_r around 0.5 was a good estimate. We have used this value.

The angular momentum distribution has been taken as

$$P(l)\,dl = \frac{2l}{l_{\max}^2}\,dl \quad \text{for } l < l_{\max},$$
$$P(l)\,dl = 0 \qquad \text{for } l > l_{\max}. \tag{2}$$

In a first attempt, we divided the surface $\int_0^{l_{\max}} P(l)dl$ into 10 equal areas, and for each zone we used an average value of l in order to calculate the rotational energies. These values for E_R and E_{Rf} were used in a preliminary calculation of Γ_f/Γ_n as a function of E_R.

For example, Table II shows that the excitation energy for which $P(7n)$, the probability of evaporating seven neutrons, is largest is 104 MeV. Each step of the evaporation chain was considered and excitation energies were calculated by subtracting from E^* the values of $S_n + \epsilon_n$, where ϵ_n is the average neutron kinetic energy, 5 MeV. Starting with the compound nucleus ^{204}Po, Γ_f/Γ_n was calculated for all succeeding nuclides down to ^{198}Po, with excitation energies ranging from 100 MeV down to 15 MeV for the last isotope. $P(7n)$ is thus obtained by adding the results obtained for each of the 10 zones as

$$P(7n) = \frac{1}{10}\sum_{k=1}^{k=10}\left\{\prod_{i=1}^{i=7}\left(\frac{\Gamma_{ni}}{\Gamma_{ni}+\Gamma_{fi}}\right)_{E_R{}^k}\right\}. \tag{3}$$

Such a calculation shows that, for the largest rotational energies, Γ_f is so large that there is no contribution to the desired residual nuclei. Therefore a limit is found above which all the events go into fission. In the case of ^{204}Po excited to 100 MeV, this limit corresponds to approximately $40\hbar$.

In a second stage of the calculation we only considered that region of the angular momentum distribution for which the probability of producing a given residual nucleus was not negligibly small. In this calculation the surface was divided into 20 new areas which represent more accurately that part of the distribution which contributes to the production of the residual nuclei of interest. The results of the calculations are summarized in Table III.

---

*Guggenheim Memorial Fellow at Institut de Physique Nucléaire, Orsay, France, 1971–72; supported in part by the U. S. Atomic Energy Commission.

[1]A. Siivola as quoted by P. Eskola, Ark. Fys. 36, 477 (1967); also Joint Institute for Nuclear Research, Dubna Report No. P7-3202, 1967 (unpublished), p.89.

[2]N. I. Tarantin, A. P. Kabachenko, and A. V. Demyanov, Joint Institute for Nuclear Research, Dubna Report No. P154706, 1969 (unpublished).

[3]H. Gauvin, Y. Le Beyec, M. Lefort, and N. T. Porile, Phys. Rev. Lett. 29, 958 (1972).

[4]L. C. Northcliffe and R. F. Schilling, Nucl. Data A7, 233 (1970).

[5]C. F. Williamson, J. P. Boujot, and J. Picard, Centre à l'Energie Atomique CEA Report No. R3042, 1966 (unpublished).

[6]R. D. MacFarlane and R. D. Griffoen, Nucl. Instrum. Methods 24, 461 (1963); R. D. MacFarlane, R. A. Gough, N. S. Oakey, and D. F. Torgerson, *ibid.* 73, 285 (1969).

[7]Y. Le Beyec, M. Lefort, and M. Sarda, Nucl. Phys. A192, 405 (1972); M. Sarda-Gugliermina, thèse 3ème cycle, Institut de Physique Nucléaire, Orsay, 1972 (unpublished).

[8]C. M. Lederer, J. M. Hollander, and I. Perlman, *Table of Isotopes* (Wiley, New York, 1967), 6th ed.

[9]H. Gauvin, R. L. Hahn, Y. Le Beyec, M. Lefort, and J. Livet, Nucl. Phys. A208, 360 (1973).

[10]W. D. Myers and W. J. Swiatecki, Nucl. Phys. 81, 1 (1966).

[11]J. Livet, thèse 3ème cycle, Institut de Physique Nucléaire, Orsay, 1973 (unpublished).
[12]Y. LeBeyec and M. Lefort, Ark. Fys. 26, 183 (1967).
[13]J. R. Grover and J. Gilat, Phys. Rev. 157, 802 (1967); J. Gilat and J. R. Grover, Phys. Rev. C 3, 734 (1971).
[14]J. Galin, B. Gatty, D. Guerreau, C. Rousset, U. C. Schlotthauer-Voos, and X. Tarrago, Institut de Physique Nucléaire, Orsay, Report No. IPNO-RC-73-03 (unpublished).
[15]G. T. Garvey, W. J. Gerace, R. L. Joffe, I. Talmi, and I. Kelson, Rev. Mod. Phys. Suppl. 41, S1 (1969).
[16]N. Zeldes, A. Grill, and A. Simievic, K. Dan. Vidensk. Selsk. Mat.-Fys. Skr. 3, No. 5 (1967).
[17]J. Huizenga and R. Vandenbosch, in *Nuclear Reactions*, edited by Endt and Demeur (North-Holland, Amsterdam, 1962), Vol. II. Nuclear Fission.
[18]Y. Le Beyec, M. Lefort, and J. Péter, Nucl. Phys. 88, 215 (1966).